Neuroplasticity predicts outcome of optic neuritis independent of tissue damage

Running head title: Damage and recovery in optic neuritis

Thomas M Jenkins MRCP,[1] Ahmed T Toosy PhD,[1] Olga Ciccarelli PhD,[1] Katharine A Miszkiel FRCR,[2] Claudia A Wheeler-Kingshott PhD,[3] Andrew P Henderson FRACP,[4] Constantinos Kallis PhD,[3,6] Laura Mancini PhD,[2] Gordon T Plant MD,[5,7] David H Miller MD,[4,5] Alan J Thompson MD[1,5]

[1]Department of Brain Repair and Rehabilitation, [2]Lysholm Department of Neuroradiology, [3]NMR Research Unit, [4]Department of Neuroinflammation, UCL Institute of Neurology, University College London and [5]National Hospital for Neurology and Neurosurgery, Queen Square, London, WC1N 3BG, [6]Medical Statistics Unit, London School of Hygiene and Tropical Medicine and [7]Moorfields Eye Hospital, City Road, London, EC1V 2PD, United Kingdom.

Correspondence to: Professor A. J. Thompson, Department of Brain Repair and Rehabilitation, UCL Institute of Neurology, Queen Square, London, WC1N 3BG. Telephone: 0845 155 5000 ext 724152. Email: a.thompson@ion.ucl.ac.uk

No. of characters in title: 79
No. of characters in running head: 37
No. of words in abstract: 230
No. of words in manuscript: 5188
No. of color figures: 4
No. of tables: 6

Objectives: To determine whether lateral occipital complex (LOC) activation with functional magnetic resonance imaging (fMRI) predicts visual outcome after clinically isolated optic neuritis (ON). To investigate the reasons behind good recovery following ON, despite residual optic nerve demyelination and neuroaxonal damage.

Methods: Patients with acute ON and healthy volunteers were studied longitudinally over 12 months. Structural MRI, visual evoked potentials (VEPs) and optical coherence tomography (OCT) were used to quantify acute inflammation, demyelination, conduction block, and later to estimate remyelination and neuroaxonal loss over the entire visual pathway. The role of neuroplasticity was investigated using fMRI. Multivariable linear regression analysis was used to study associations between vision, structure, and function.

Results: Greater baseline fMRI responses in the LOCs were associated with better visual outcome at 12 months. This was evident on stimulation of either eye (P=0.007 affected, and P=0.020 fellow eye), and was independent of measures of demyelination and neuroaxonal loss. A negative fMRI response in the LOCs at baseline was associated with a relatively worse visual outcome. No acute electrophysiological or structural measures, in the anterior or posterior visual pathways, were associated with visual outcome.

Interpretation: Early neuroplasticity in higher visual areas appears to be an important determinant of recovery from ON, independent of tissue damage in the anterior or posterior visual pathway, including neuroaxonal loss (as measured by MRI, VEP and OCT) and demyelination (as measured by VEP).

Most patients with acute idiopathic demyelinating optic neuritis (ON) make a good visual recovery. However, 5-10% recover poorly,[1] and many more notice residual qualitative deficits.[2] For these people, there are no effective treatments to improve vision. Understanding the mechanisms underlying damage and repair in demyelinating disease of the central nervous system is important in order to devise better therapies. In addition, predictors are required which identify patients with a poor visual prognosis, so that they can be prioritized for clinical trials of experimental therapies, such as neural stem cells.[3]

Although ON is used to study demyelination, the mechanisms of damage and repair in ON are incompletely understood. During the acute phase, there is inflammation, demyelination and conduction block in the optic nerve.[4] Over subsequent weeks, inflammation resolves and electrical conduction, and consequently vision, improve, although there is frequently evidence for persistent optic nerve demyelination.[5,6] Neuroaxonal loss also occurs, and optic atrophy generally ensues.[7,8] Evidence for remyelination, suggested by shortening of visual evoked potential (VEP) latency, may be seen later, but generally not until clinical recovery is almost complete.[5] It is therefore of interest that most patients make good visual recoveries, considering the frequency of residual tissue damage, including axonal loss, a phenomenon usually associated with permanent disability in demyelinating diseases.[9] This dissociation between optic nerve tissue damage and degree of visual recovery can be partially explained by the large number of axons in the optic nerve, in excess of the critical threshold necessary to maintain function (*neuroaxonal redundancy)*. An independent hypothesis implicates compensatory reorganization of cortical processing, and is known as *adaptive neuroplasticity*. Evidence for neuroplasticity following ON has been reported by

functional MRI (fMRI) studies.[10-12] In particular, Toosy *et al* reported evidence for adaptive plasticity early after ON within the lateral occipital complexes (LOCs), after accounting for potentially confounding optic nerve structural pathology.[10] However, many aspects of the mechanism underlying this plasticity remain unclear, such as the role of the fellow eye, the interaction of different levels of the visual processing hierarchy in response to insult[13] and the relationships to concurrent processes of structural damage and repair across the whole visual axis.

Currently, it is not possible to predict reliably which patients will fail to recover from an attack of ON. A longer gadolinium-enhancing lesion in the optic nerve during the acute episode was associated with worse visual outcome in one study,[14] but not in another.[15] Worse visual acuity at one month,[16] a less steep initial gradient of improvement of acuity, and smaller amplitude VEPs during the recovery phase[14] have been associated with worse visual prognosis, but are not helpful at the time of diagnosis. Similarly, whilst thinning of `the retinal nerve fibre layer (RNFL),[17,18] optic nerve atrophy,[7,19] and reduced magnetization transfer ratio (MTR) of the optic nerve[7] have been associated with poor outcome, they are not evident until months or years after the event.

The aims of this serial ON study were in part hypothesis driven, based on previous reports implicating the LOCs in neuroplasticity. We hypothesized that early LOC activation was significantly associated with visual outcome after accounting for markers of anterior and posterior visual pathway damage. We also investigated the relative contributions of optic nerve myelination and neuroaxonal damage to visual outcome after ON. We were able to address these questions through a comprehensive structural and functional imaging protocol over time. Structural/diffusion MRI techniques assessed

optic nerve and radiation involvement. VEP latency and amplitude reflected myelination and surviving axonal populations, respectively. Optical coherence tomography (OCT) assessed macular volume and RNFL thickness, and visual fMRI investigated neuroplasticity.

Subjects and Methods

Participants

Consecutive patients with acute unilateral clinically isolated ON were recruited from Moorfields Eye Hospital. Patients with multiple sclerosis, bilateral ON, or other chronic neurological conditions were excluded. Patients with incidental inflammatory lesions in the brain, identified on MRI scans performed after recruitment, were included in the study. Patients were invited for clinical assessment, VEPs, structural and functional MRI, on the same day, within a month from onset and three, six and 12 months later. In addition, at one year follow-up patients were invited for OCT imaging. A summary of the different techniques used is shown in Figure 1.

Healthy age and sex matched controls were recruited at baseline, and were invited for follow-up MRI at each time-point, and one VEP and OCT assessment. All subjects gave informed written consent. The study was approved by the local Ethics Committee.

Visual testing

Each patient's best corrected visual acuity, using glasses and pinhole correction if necessary, was measured using a retro-illuminated Early Treatment Diabetic Retinopathy

Study (ETDRS) Chart. Scores were recorded as the 4m logarithm of the minimum angle of resolution (logMAR) acuity.[20] Higher logMAR scores indicated worse vision.

Electrophysiology

Whole and central field pattern-reversal VEP studies were performed. Details of the parameters have been described previously.[21]

Optical coherence tomography

OCT imaging was acquired with a Stratus OCT Model 3000 (Carl Zeiss MediTec, Dublin, Ca, USA). The Model 3000 assesses signal strength and assigns a score. Images were only accepted if the score was >7/10, and the inter-eye difference was <2/10, and RNFL images and macular thickness maps were then calculated, according to previously described protocols.[22] All scans were performed by the same operator (AH). OCT became available on-site during the course of the study, at which point six patients with longitudinal follow-up had passed the 12 month time-point. Therefore, these patients and one control did not have an OCT examination.

MRI acquisition and analysis

Two 1.5T GE Medical Systems scanners (Milwaukee, WI) were used to acquire MRI data, using an 8-channel receive-only head-coil. The scanners were chosen based on their dedicated setup. Structural imaging of the optic nerves and brain was performed in all subjects with a 1.5-T Signa Echospeed MRI system, with a maximum gradient strength of $33mTm^{-1}$, whilst functional imaging was performed, on the same day, on a 1.5-T Signa

Excite whole-body MRI system, with a lower gradient strength of 22mTm^{-1}, but with the equipment for paradigm presentation for visual stimulation.

Structural MRI

OPTIC NERVES

(1) A coronal-oblique fast spin-echo sequence (TR 2300ms, TE 68ms, 2 excitations, echo train length 8, matrix size 512x384, field of view (FOV) 24x18cm, 16 contiguous 3mm slices) was acquired to calculate lesion length, which was determined by an experienced neuroradiologist (KM), blinded to image identity and side affected, by multiplying the number of consecutive slices of optic nerve returning abnormal signal by the slice thickness. The intra-observer reproducibility coefficient of variation was 2.8%.

(2) Post triple-dose gadolinium-enhanced coronal-oblique fat-saturated T1-weighted spin echo was acquired in patients only (TR 600ms, TE 20ms, 1 excitation, matrix size 256x192, FOV 24x18cm, 16 contiguous 3mm slices).

(3) Coronal-oblique FLAIR imaging (TR 2500ms, TE 12.7ms, TI 995ms, 6 excitations, echo train length 6, matrix size 512x384, FOV 24x18cm, 16 contiguous 3mm slices) was performed to obtain the optic nerve cross-sectional area, which was calculated by a single, blinded observer (TJ), from five contiguous slices anterior from the orbital apex,[23] using a semi-automated contouring technique.[24] The intra-observer reproducibility coefficient of variation was 4.6%. In order to account for inter-individual variability, the ratio of affected to fellow nerve area was calculated.

OPTIC RADIATIONS

(1) Axial-oblique dual-echo fast spin-echo of the whole brain (TR 2000ms, TE 17ms/102ms, echo train length 8, matrix size 256x256, FOV 24x18cm, 28 contiguous 5mm slices) were used by TJ to calculate the optic radiation lesion load, after lesions were identified by KM, using standard anatomical landmarks to identify the optic radiations. Intra-observer coefficient of variation was 2.6%.

(2) Diffusion tensor imaging (DTI) of the optic radiations and occipital lobe was obtained using an optimized single-shot, cardiac-gated, diffusion-weighted echo-planar imaging sequence (TR 10 RR~11-13s, TE 82ms, 1 excitation, matrix size 96x96 (reconstructed to 128x128), FOV 22x22cm^2, in-plane resolution 2.3x2.3mm^2 (reconstructed to 1.7x1.7mm^2), 30 contiguous 2.3mm slices, parallel to the AC-PC line, diffusion-weighting gradients applied along 61 distributed directions,[25] b=1200s/mm^2, optimised for white matter, and seven interleaved non-diffusion-weighted b0 scans, acquisition time 10-15 minutes, depending on cardiac cycle). One additional b0 volume was acquired, covering the whole brain (60 slices, extended from the original 30), to assist coregistration of partial brain diffusion data to whole brain fMRI data, which was necessary for tractography. Head motion and eddy-current induced distortions were corrected and the diffusion tensor was then calculated on a pixel-by-pixel basis, using FSL tools (http://www.fmrib.ox.ac.uk/fsl/).

The optic radiations were reconstructed, using the FSL probabilistic tractography algorithm (http://www.fmrib.ox.ac.uk/fsl/fdt/fdt_probtrackx.html).[26,27] Seed-points were located in each Meyer's loop using fMRI data (see Supplementary Material (1) for details). The mean fractional anisotropy (FA) within the tractography-derived tract was obtained for each side, in each subject, at each time-point.

OCCIPITAL CORTEX

Three-dimensional FSPGR of the whole brain was acquired (TR 14.3ms, TE 5.1ms, 1 excitation, matrix size 256x128, FOV 31x31cm, 156 1.2mm slices).

The images were analyzed with FreeSurfer software (http://surfer.nmr.mgh.harvard.edu), in which they were reconstructed as 1x1x1mm axial images, and the brain extracted. The skull-strip was assessed visually in all cases, and manual correction performed if necessary, by a single observer (TJ), blinded to image identity. Fully automated cortical parcellation was then performed, and pericalcarine surface area, volume and cortical thickness estimates obtained.[28-31]

Functional MRI Imaging

FMRI data were acquired in four runs, using a T2*-weighted echo-planar imaging sequence, with 38 axial-oblique slices covering the whole brain, parallel to the AC-PC line (TR 3950ms, TE 50ms, matrix size 64x64, FOV 20cm, slice thickness 2mm, 1mm gap).

The subjects viewed visual stimuli, comprising blocks of flickering chromatic checkerboards, alternated with blocks of grey background, presented on a projection screen, through plano chromatic filter goggles, to facilitate maintenance of attention and fixation, and test both eyes in the same run.[32] To confirm attention, the subjects were instructed to fixate a central cross, asked to press a button when it changed, and responses were recorded (see Supplementary Material (2) for details). The patients responded correctly to the fixation cross changing 87.5% of the time, and controls 97% of the time, indicating generally good attention and fixation.

Statistical parametric mapping software was used for processing the data at each time-point (SPM5, Wellcome Department of Cognitive Neurology, London, UK). Each fMRI series was realigned, normalized to MNI stereotactic space and smoothed, using an 8mm isotropic Gaussian kernel. Realignment parameters and time derivatives were entered as covariates into the model, together with the times when subjects pressed the button. For each subject, first level +1 contrasts were specified separately for affected and fellow eyes. The resulting contrast images were entered into separate one-sample t-tests at the second level for affected and fellow eyes, with side of stimulation entered as a covariate.

Based on previous work,[10-12] regions-of-interest were specified in both LGNs, bilateral primary visual cortex, both LOCs and bilateral cuneus (see Supplementary Material (3) for details on the regions-of-interest). Mean parameter estimates reflecting the blood oxygenation level dependent (BOLD) signal were extracted using the "MarsBar" SPM toolbox,[33] for each subject, at each time-point.

Statistical analysis

All statistical analysis was performed using Stata-9.2 (StataCorp, Texas, USA), unless otherwise stated. The analysis proceeded in several stages, detailed below. $P<0.05$ was chosen to represent statistical significance.

(1) Longitudinal analysis

To explore longitudinal changes, mixed effects models were specified separately, for each variable, in patients and controls. In addition, for variables in which changes were significant, the median and interquartile ranges were reported for change between

baseline and 12 months. Differences in the variables available at 12 months for patients and controls (i.e. VEP and OCT parameters), between patients affected and fellow eyes, and a randomly selected control eye, were assessed using unpaired t-tests.

(2) Identifying associations between visual outcome and baseline (or 12 month) variables

Visual outcome was defined as logMAR (affected eye) at 12 months. To identify baseline predictors of visual outcome, regression models were separately specified, entering baseline structural MRI, VEP and fMRI measures, and demographic parameters as independent variables, with logMAR acuity at 12 months as the dependent variable. The model was repeated, in turn, for each independent variable. The number of days from symptom onset to initial assessment and acuity in the fellow eye were included as covariates in the model, to allow for any inter-individual differences in the stage of evolution of pathology and pre-morbid acuity. To identify variables measured at 12 months that were associated with visual outcome at 12 months, regression models were specified, with logMAR acuity at 12 months as the dependent variable, and the 12 month structural MRI, VEP, OCT and fMRI measures as independent variables. For the OCT data, fellow eye parameters were also added to the model, to adjust for normal inter-individual variability.[34]

(3) Relationship between baseline LOC responses and visual outcome

As a result of significant associations between LOC activation and visual outcome (see Results) the two variables were plotted. A threshold of affected eye LOC fMRI response was visually determined that would dichotomize visual outcome into two groups of better relative outcome and worse relative outcome with high sensitivity and specificity.

4) Inter-variable structure-function relationships and visual outcome

The five significant variables found in analysis (2) were investigated further. Two of these were affected and fellow eye LOC fMRI responses. The others were baseline acuity, age and 12 month macular volume. Multivariable regression models were specified, with logMAR at 12 months as the dependent variable as before, except now each of the other demographic, structural and functional variables was also added, in turn, to the model, to assess its influence on the relationship between the variable of interest and logMAR at 12 months. This was performed for the dependent variables separately at baseline and 12 months. These analyses involved numerous statistical tests and raised the issue of multiple comparisons. Although there is no ideal method to address this for the family wise error rate (FWER), we felt it would be prudent to report P values both uncorrected and corrected for multiple comparisons (by variable), using the relatively conservative Holm procedure.[35,36] For analyses of LOC activation, based on our *a priori* hypothesis of their neuroplasticity-related contribution to visual outcome, greater attention should be paid to the uncorrected P values (first two columns of tables 5 and 6).

Results

Patient characteristics and dataset

Twenty-eight patients and ten age and sex-matched controls were recruited at baseline (Table 1). The median duration from symptom onset to baseline assessment was 22 days

(range 7-34). Twenty five patients and eight controls attended the follow-up visits, as summarized in Table S1 (Supplementary Material).

1) Longitudinal analysis

Over the year, patients' vision improved by a median of 0.42 logMAR units (inter-quartile range (IQR) 0.11, 1.38). 74% of patients recovered acuity to logMAR<0.2 (better than Snellen equivalent 20/32). Optic nerve lesion length increased by 9mm over the year (IQR 6, 13) and optic nerve area ratio decreased by 25% (IQR 10%, 38%). The median increase in optic radiation lesion load was 15mm^2 (IQR 0, 78). VEP amplitude improved by 2.63μV (IQR -0.49, 4.44) and VEP latency reduced by 11.7ms (IQR 5.6, 20.2). For some variables, the rates of change varied over time (Table 2, Figure 2).

In controls, there were no significant changes over time in the variables examined.

Longitudinal changes in fMRI responses in patients are plotted in Figure 3. In lower visual areas (LGN and primary visual cortex), affected eye responses showed the greatest increase over the first three months, and the observed decreases in fellow eye responses did not reach statistical significance. In contrast, in higher visual areas (LOCs and cuneus), there were significant decreases in fellow eye responses over time. There were no changes in controls between baseline and 12 months.

At 12 months, macular volume and RNFL thickness were reduced, and VEP latency was prolonged in the patients' affected eyes, compared to controls (Table 3). There were no significant differences in fellow eye parameters between patients and controls.

2) Associations between visual outcome and baseline (or 12 month) variables

The strongest baseline predictor was fMRI response in the LOCs, on stimulating the affected eye (Table 4): greater fMRI activity was associated with better logMAR acuity at 12 months (P=0.007). There was also an association in the same region between fMRI response and visual outcome when the fellow eye was stimulated (P=0.020). No acute structural measures were significantly associated with visual outcome. There was an association with the initial severity of visual loss and a weak influence of age, with older patients tending to have better acuities at 12 months. At 12 months, the only significant result was a weak association between smaller macular volume and worse outcome (Table 4). An increase in macular volume of $1mm^3$ corresponded to an improvement in logMAR acuity of 0.33 (approximately three lines on the chart).

3) Relationship between baseline LOC responses and visual outcome

Figure 4 demonstrates increasing baseline LOC responses associated with better visual outcome. Visual recovery could be divided into a better relative outcome group (logMAR <0.2, Snellen equivalent better than 20/32), or a worse relative outcome group, on the basis of thresholding the baseline LOC activation. Baseline LOC fMRI responses were positive in the better relative outcome recovery group (mean parameter estimate 0.57 [95%CI 0.16, 0.98]) and negative in the worse relative outcome group (mean -0.59 [95%CI -1.1, -0.023], t=3.28, P=0.004). For an individual patient, a negative baseline LOC response was associated with a logMAR acuity of 0.2 or worse (Snellen equivalent worse than 20/32) a year after ON, with a sensitivity of 83% (95%CI 36%, 100%), specificity of 88% (95%CI 64%, 99%) and accuracy of 87% (95%CI 66%, 97%).

Seventeen patients were in the group with relatively better outcome whereas six were in the other group.

4) Inter-variable structure-function relationships and visual outcome

There were complex interactions between the previously identified variables of interest and the other structural and functional variables, representing pathology in the acute phase (Table 5) and residual damage at 12 months (Table 6). However, the association between baseline affected eye fMRI response in the LOCs and visual outcome was independent of any demographic, structural or electrophysiological factors, from either the baseline or 12 month time-points. The relationship between baseline fellow eye fMRI response in the LOCs and visual outcome also generally maintained significance, although not as consistently as the affected eye LOC response.

Neither baseline visual acuity nor age survived the models that adjusted for affected eye fMRI response in the LOCs, nor the models that adjusted for fellow eye responses in the LOCs. The relationship between macular volume at 12 months and visual outcome lost significance following adjustment for several of the other variables, notably baseline acuity and age.

Effect of outlier

Patient 22 had significantly worse residual visual dysfunction than the rest of the group (Table 1, Figure 4). We repeated the analyses without this subject, and all associations remained significant, except for macular volume.

Discussion

The most important finding from this study is the direct association between acute fMRI responses in the LOCs and visual outcome, evident on stimulation of either eye. Visual outcome was also associated with the severity of acute visual loss and 12 month macular volume, but not with any other markers of neuroaxonal loss in the optic nerve, demyelination, or damage to the posterior pathways. These data suggest that early adaptive neuroplasticity in the LOCs is an important determinant of visual recovery in clinically isolated ON, independent of measures of tissue damage.

1) Longitudinal analysis

The changes in clinical, structural and electrophysiological variables are consistent with the known pathophysiology of ON. Acutely, oedema, inflammation, demyelination and conduction block were evident and, as they resolved, vision improved. Despite clinical recovery, there was evidence of ongoing tissue damage, such as progressive lengthening of the optic nerve lesion, which may represent secondary tract degeneration. At 12 months, VEP latencies demonstrated persistent demyelination, despite evidence for remyelination between six and 12 months. Neuroaxonal loss in the optic nerve was evident from a reduction in macular volume and RNFL thickness, in addition to optic nerve atrophy. FMRI responses in lower visual areas improved over the first three months, in parallel with vision, and consistent with an increased afferent input. Responses in higher visual areas were more complex, with dynamic changes evident on fellow eye stimulation over time.

2) Associations between visual outcome and baseline (or 12 month) variables

The strongest predictor of visual outcome was the fMRI response in the LOCs, and this was evident on stimulation of either eye. The LOCs are higher order visual areas, located within the ventral processing stream, involved in identification and recognition of objects in the physical world. They have previously been identified as potentially important areas for neuroplasticity in ON.[10] Toosy *et al* used an indirect methodology, in a longitudinal cohort, to correlate residual variance in clinical function with fMRI response in voxels throughout the whole brain, after accounting for acute optic nerve inflammation. The LOCs correlated with the residual variance in clinical function, only at the baseline time-point. A later cross-sectional study reported changes in the LOCs later in the recovery process.[11] A longitudinal study reported evidence for primary neuroplasticity in the LGN,[12] although the authors also considered whether the observed changes might represent back-projection from cortical areas. The present study is the first to investigate neuroplasticity in the context of complicating structure-function interactions, involving both the anterior and posterior pathways, and the first to take into account both acute inflammation and residual tissue damage.

A reduction in macular volume (demonstrated by OCT at 12 months) is most likely to represent loss of retinal ganglion cells, secondary to axonal damage in the optic nerve[37] (although macular volume loss is not retinal layer-specific), and supports a role for the extent of neuroaxonal loss in determining clinical outcome. However, we could not confirm the previously reported association between RNFL thickness and visual loss.[17,18,38] This may be because of differences in the study cohorts; all our patients had

clinically isolated ON, unselected for visual function. We also found no association between optic nerve atrophy on MRI and visual outcome. Previous studies have reported either modest correlations between visual outcome and tissue loss in the optic nerve[7,19] or none.[8] Of the hypotheses postulated to explain this dissociation between tissue loss in the optic nerve and clinical function, there was no evidence for an impact of damage within the posterior pathways. The restricted clinical impact despite macular volume loss may represent a degree of neuroaxonal redundancy, but the relatively strong fMRI associations suggest that acute grey matter plastic changes appear to exert a greater influence.

Increasing age was also associated with a better visual outcome. The reasons for this are not clear from this study.

3) Relationship between baseline LOC responses and visual outcome

A negative affected eye fMRI response in the LOCs appears to predict a worse relative outcome, whilst a positive response is associated with a better relative outcome. This threshold effect suggests a genuine physiological role for compensatory plasticity in this cohort. A positive fMRI response may represent synaptic reorganization or dendritic arborization, contributing to recovery. Conversely, negative responses may indicate failure of neuroplastic mechanisms, with a resulting visual deficit. In this context, deactivation might even reflect maladaptive change, and this merits further study. Acutely, a negative fMRI response in the LOCs appears to help identify individuals with a less favorable visual prognosis, and the results we report for sensitivity, specificity and accuracy are promising from a clinical perspective, although the confidence intervals are

wide, and the degree of residual visual dysfunction in the group with relatively worse recovery was variable. Further studies in larger groups of patients with ON are required to determine whether these results are generalizable.

It is interesting that the association between visual outcome and fMRI response in the LOCs was evident on stimulation of either eye. Abnormal fellow eye responses have been reported previously, although their role in recovery was unclear. Toosy *et al* found that acute fMRI responses in the fellow eye correlated with acute vision in the affected eye.[10] Our findings extend these results, by associating fellow eye responses with visual recovery. This might be explained through a mechanism of subclinical pathology in the fellow optic nerve. However, there is little evidence for this from the present study, as only one subject had an asymptomatic optic nerve lesion, and there were no differences from controls in the other structural and electrophysiological measures. Therefore, our findings suggest that cortical fMRI responses are remodulated holistically, in response to pathological insult, and contribute to recovery. This may be of practical use in future studies of plasticity in patients with severe visual loss, when it may be difficult to detect any fMRI response from the affected eye, due to acute conduction block.

After the acute episode, fMRI responses within the LOCs, in either the affected or fellow eye, were no longer associated with visual outcome, suggesting that the acute phase is most important in terms of brain reorganization.[39]

4) Inter-variable structure-function relationships and visual outcome

The relationship between affected eye (and, to some degree, fellow eye) fMRI activity in the LOCs and visual outcome remained independent of measures of acute inflammation, residual demyelination and neuroaxonal loss. The severity of acute visual loss was associated with subsequent recovery, and some of the variance in visual outcome attributable to fMRI responses in the LOCs was also explained by this variable, although fMRI response remained a stronger predictor. This collinearity was not surprising, as a two-way relationship exists between acuity and fMRI response; on one hand, a reduced neuronal input results in a smaller response whilst, on the other hand, plastic reorganization may influence acuity. However, the association between baseline fMRI response in the LOCs and visual recovery cannot be explained solely through a mechanism of severity of acute visual loss. This alternative mechanism should operate via the primary visual areas and when the affected eye is stimulated. However, firstly, affected eye LOC activity was a stronger predictor than the primary visual areas which were non-significant (Table 4). Secondly, it would be difficult to physiologically explain the significant associations between baseline *fellow* eye LOC activity and 12 month visual outcome purely on the basis of reduced visual acuity (resulting from impaired afferent stimuli through the affected eye only) at baseline. Thirdly, LOC fMRI activity generally maintained greater levels of significance even after incorporating other interaction variables (for baseline and 12 months) into the model (Tables 5 and 6) whilst baseline acuity did not, implying a more critical role for LOC activity in predicting visual outcome. Our results still imply, however, that higher visual areas, such as the LOCs, are not robust to disruption of visual input, a point which has been debated following contrasting results from two previous studies.[11,12]

The relationships between visual outcome, baseline acuity, age, and 12 month macular volume were more complex, and structure-function interactions were evident, influencing associations with vision.

Two potential sources of error were investigated *post-hoc*. Firstly, we determined whether the baseline fMRI responses in the LOCs were influenced by between-subject variation in attention, potentially related to differences in baseline acuity. However, a regression analysis found no association between attention scores and baseline acuity (P=0.860). Secondly, we considered whether it was appropriate to consider linearity for the relationship between baseline and final acuity in the multivariable regression analysis. We performed separate regression analyses to respectively investigate three relationships between baseline and final acuity: 1) linear, 2) a combination of linear and quadratic and 3) logarithmic. The strongest association was found to be linear (P=0.031). No significant associations were found for quadratic (P=0.487) and logarithmic (P=0.142) terms. We then extracted the unstandardized residuals after regression between baseline and final acuity (assuming the linear relationship). These residuals were, in turn, regressed with baseline lateral occipital complex (LOC) activation for the affected (P=0.227) and fellow (P=0.137) eye respectively. These non-significant P values imply that there are no residual confounding factors between baseline acuity predicting final acuity that relate to LOC activation and, consequently, assuming linearity whilst controlling for baseline acuity in the multivariable regression was probably sufficient.

Methodological considerations

There are several methodological considerations for our study. Firstly is the issue of correcting for multiple comparisons. This study comprised in part hypothesis-driven aims. The key results suggesting LOC neuroplasticity are based on our *a priori* hypothesis and so, for these, we felt multiple comparisons corrections were less essential and that the reader could place greater weight on the uncorrected P values (first two columns in Tables 5 and 6). Issues of multiple comparisons correction for family-wise error rate (FWER) occur perennially in research. Unfortunately, there is no ideal method to adjust for them. Conventional approaches that control the FWER, such as Bonferroni, Holm and Sidak, have several disadvantages.[40,41] They are intrinsically conservative, risking an increase in type II errors, they assume that the tests are independent (which is usually not the case) and are concerned with the general null hypothesis (that all null hypotheses are true simultaneously), which is rarely of interest to researchers. In these contexts where there is considerable biological similarity in the relationships assessed by individual tests, a biological pattern of moderately significant results (or multiple convergent associations) is very unlikely to occur by chance, and applying a naïve FWER multiple comparisons correction may eliminate genuine associations. As an example, for the LOC analysis in Table 5, 28 tests were performed. Twenty three significant results (uncorrected) are tabulated, making it extremely unlikely that they have all arisen by chance. What is important in these contexts is to highlight the patterns, and to treat with great caution any moderately significant individual results which are biologically isolated. Nevertheless, for the exploratory analyses in Tables 5 and 6, we were aware that the large number of tests performed represents a limitation of our dataset, and addressed this potential interpretational difficulty by applying a Holm correction. We

reported both the uncorrected and corrected P values, so that the relative statistical strength of each association was clear. We felt this was a sensible way to address the multiple comparisons issue.

Secondly, there were some missing data-points, which is difficult to avoid when conducting a comprehensive longitudinal study. In a minority of subjects, it was not possible to obtain all tests on the same day (Table S1). However, we addressed these problems during the analysis stage, by using mixed effects models which allow for missing time-points, and maximize efficient use of the available data, and by including time-to-test variables in the multivariable regression models.

Thirdly, in order to minimize scanning times, the LOCs and primary visual cortex were defined on the basis of published coordinates, rather than using a localizer task and retinotopic mapping, which better account for inter-subject variability. However, the longitudinal fMRI data shown in Figure 3 suggest that the estimates from our study were accurate, as changes over time were captured that appear physiologically feasible, and consistent with previous studies.

In summary, this study identified an association between fMRI activity in the LOCs during acute ON and visual outcome, which was independent of measures of optic nerve inflammation, myelination and neuroaxonal loss. These data suggest that early neuroplasticity contributes to recovery from clinically isolated ON, and helps explain the dissociation between optic nerve tissue loss and visual recovery, independent of optic nerve myelination, the extent of neuroaxonal loss, or posterior pathway pathology.

References

1. Beck RW, Gal RL, Bhatti MT, et al. Visual function more than 10 years after optic neuritis: experience of the optic neuritis treatment trial. Am J Ophthalmol 2004;137:77-83.

2. Cleary PA, Beck RW, Bourque LB, et al. Visual symptoms after optic neuritis. Results from the Optic Neuritis Treatment Trial. J Neuroophthalmol 1997;17:18-23.

3. Kolappan M, Connick P, Compston A, et al. Optic neuritis as a sentinel lesion to study neuroprotection and repair in a trial of autologous mesenchymal stem cells in multiple sclerosis (Abstract). Multiple sclerosis 2008;14:S1:284.

4. Smith KJ, McDonald WI. The pathophysiology of multiple sclerosis: the mechanisms underlying the production of symptoms and the natural history of the disease. Philos Trans R Soc Lond B Biol Sci 1999;354:1649-1673.

5. Jones SJ. Visual evoked potentials after optic neuritis. Effect of time interval, age and disease dissemination. J Neurol 1993;240:489-494.

6. Hickman SJ, Toosy AT, Jones SJ, et al. Serial magnetization transfer imaging in acute optic neuritis. Brain 2004;127:692-700.

7. Inglese M, Ghezzi A, Bianchi S, et al. Irreversible disability and tissue loss in multiple sclerosis: a conventional and magnetization transfer magnetic resonance imaging study of the optic nerves. Arch Neurol 2002;59:250-255.

8. Hickman SJ, Toosy AT, Jones SJ, et al. A serial MRI study following optic nerve mean area in acute optic neuritis. Brain 2004;127:2498-2505.

9. Miller DH, Barkhof F, Frank JA, et al. Measurement of atrophy in multiple sclerosis: pathological basis, methodological aspects and clinical relevance. Brain 2002;125:1676-1695.

10. Toosy AT, Hickman SJ, Miszkiel KA, et al. Adaptive cortical plasticity in higher visual areas after acute optic neuritis. Ann Neurol 2005;57:622-633.

11. Levin N, Orlov T, Dotan S, et al. Normal and abnormal fMRI activation patterns in the visual cortex after recovery from optic neuritis. Neuroimage 2006;33:1161-1168.

12. Korsholm K, Madsen KH, Frederiksen JL, et al. Recovery from optic neuritis: an ROI-based analysis of LGN and visual cortical areas. Brain 2007;130:1244-1253.

13. Kolappan M, Henderson A, Jenkins T, et al. Assessing structure and function of the afferent visual pathway in multiple sclerosis and associated optic neuritis. J Neurol 2009;256:305-319.

14. Hickman SJ, Toosy AT, Miszkiel KA, et al. Visual recovery following acute optic neuritis-a clinical, electrophysiological and magnetic resonance imaging study. J Neurol 2004;251:996-1005.

15. Kupersmith MJ, Alban T, Zeiffer B, et al. Contrast-enhanced MRI in acute optic neuritis: relationship to visual performance. Brain 2002;125:812-822.

16. Kupersmith MJ, Gal RL, Beck RW, et al. Visual function at baseline and 1 month in acute optic neuritis: predictors of visual outcome. Neurology 2007;69:508-514.

17. Trip SA, Schlottmann PG, Jones SJ, et al. Retinal nerve fiber layer axonal loss and visual dysfunction in optic neuritis. Ann Neurol 2005;58:383-391.

18. Costello F, Coupland S, Hodge W, et al. Quantifying axonal loss after optic neuritis with optical coherence tomography. Ann Neurol 2006;59:963-969.

19. Hickman SJ, Brierley CM, Brex PA, et al. Continuing optic nerve atrophy following optic neuritis: a serial MRI study. Mult Scler 2002;8:339-342.

20. Ferris FL, III, Kassoff A, Bresnick GH, et al. New visual acuity charts for clinical research. Am J Ophthalmol 1982;94:91-96.

21. Brusa A, Jones SJ, Plant GT. Long-term remyelination after optic neuritis: A 2-year visual evoked potential and psychophysical serial study. Brain 2001;124:468-479.

22. Henderson AP, Trip SA, Schlottmann PG, et al. An investigation of the retinal nerve fibre layer in progressive multiple sclerosis using optical coherence tomography. Brain 2008;131:277-287.

23. Hickman SJ, Brex PA, Brierley CM, et al. Detection of optic nerve atrophy following a single episode of unilateral optic neuritis by MRI using a fat-saturated short-echo fast FLAIR sequence. Neuroradiology 2001;43:123-128.

24. Plummer DL. DispImage: A display and analysis tool for medical images. Rivista di Neuroradiologia 1992;5:489-495.

25. Cook PA, Symms M, Boulby PA, et al. Optimal acquisition orders of diffusion-weighted MRI measurements. J Magn Reson Imaging 2007;25:1051-1058.

26. Behrens TE, Woolrich MW, Jenkinson M, et al. Characterization and propagation of uncertainty in diffusion-weighted MR imaging. Magn Reson Med 2003;50:1077-1088.

27. Behrens TE, Johansen-Berg H, Woolrich MW, et al. Non-invasive mapping of connections between human thalamus and cortex using diffusion imaging. Nat Neurosci 2003;6:750-757.

28. Dale AM, Fischl B, Sereno MI. Cortical surface-based analysis. I. Segmentation and surface reconstruction. Neuroimage 1999;9:179-194.

29. Fischl B, Sereno MI, Dale AM. Cortical surface-based analysis. II: Inflation, flattening, and a surface-based coordinate system. Neuroimage 1999;9:195-207.

30. Fischl B, Dale AM. Measuring the thickness of the human cerebral cortex from magnetic resonance images. Proc Natl Acad Sci USA 2000;97:11050-11055.

31. Fischl B, van der KA, Destrieux C, et al. Automatically parcellating the human cerebral cortex. Cereb Cortex 2004;14:11-22.

32. Jenkins TM, Mancini L, Toosy AT, et al. A quadrant-specific monocular visual functional MRI paradigm designed to minimize attention and loss-of-fixation biases (Abstract). ISMRM 16th Scientific Meeting and Exhibition, Toronto, Canada. 2008;2460.

33. Brett M, Anton, JL, Valabregue R, et al. Region-of-interest analysis using an SPM toolbox (Abstract). 8th International conference on functional mapping of the human brain, Sendai, Japan. Neuroimage 2002;2:16.

34. Alamouti B, Funk J. Retinal thickness decreases with age: an OCT study. Br J Ophthalmol 2003;87:899-901.

35. Holm S. A simple sequentially rejective multiple test procedure. Scand J Statistics 1979;6:65-70.

36. Aickin M, Gensler H. Adjusting for multiple testing when reporting research results: the Bonferroni vs Holm methods. Am J Public Health 1996;86:726-728.

37. Quigley HA, Davis EB, Anderson DR. Descending optic nerve degeneration in primates. Invest Ophthalmol Vis Sci 1977;16:841-849.

38. Klistorner A, Arvind H, Nguyen T, et al. Axonal loss and myelin in early ON loss in postacute optic neuritis. Ann Neurol 2008;64:325-331.

39. Johansen-Berg H. Structural plasticity: rewiring the brain. Curr Biol 2007;17:141-144.

40. Perneger TV. What's wrong with Bonferroni adjustments. BMJ 1998;316:1236-1238.

41. Rothman KJ. No adjustments are needed for multiple comparisons. Epidemiology 1990;1:43-46.

42. Guye M, Parker GJ, Symms M, et al. Combined functional MRI and tractography to demonstrate the connectivity of the human primary motor cortex in vivo. Neuroimage 2003;19:1349-1360.

43. Horton JC, Landau K, Maeder P, et al. Magnetic resonance imaging of the human lateral geniculate body. Arch Neurol 1990;47:1201-1206.

44. Ciccarelli O, Behrens TE, Altmann DR, et al. Probabilistic diffusion tractography: a potential tool to assess the rate of disease progression in amyotrophic lateral sclerosis. Brain 2006;129:1859-1871.

45. Jenkinson M, Smith S. A global optimisation method for robust affine registration of brain images. Med Image Anal 2001;5:143-156.

46. Zhang Y, Brady M, Smith S. Segmentation of brain MR images through a hidden Markov random field model and the expectation-maximization algorithm. IEEE Trans Med Imaging 2001;20:45-57.

47. Thottakara P, Lazar M, Johnson SC, et al. Application of Brodmann's area templates for ROI selection in white matter tractography studies. Neuroimage 2006;29:868-878.

48. Ciccarelli O, Wheeler-Kingshott CA, McLean MA, et al. Spinal cord spectroscopy and diffusion-based tractography to assess acute disability in multiple sclerosis. Brain 2007;130:2220-2231.

49. Slotnick SD, Klein SA, Carney T, et al. Electrophysiological estimate of human cortical magnification. Clin Neurophysiol 2001;112:1349-1356.

50. Jenkins TM, Mancini L, Ciccarelli O, et al. Using structural and functional magnetic resonance imaging to explain visual loss at the onset of acute optic neuritis (Abstract). Multiple sclerosis 2008;14;S1:276.

Table 1. Patient characteristics

Patient	Age (years)	Sex	Side	LogMAR			
				Baseline	3 months	6 months	12 months
1	38	F	R	0.4			
2	27	F	L	-0.02	-0.02	0.08	0.1
3[a]	24	F	L	1.7	0.5	0.4	0.32
4	27	F	R	0.5	0.1	0	0.06
5	20	M	L	0.4	0.4	0.06	0.22
6	25	F	L	0.14	0.1	0	0.02
7	39	F	L	0.06	-0.1	0.02	-0.1
8	36	F	R	0	-0.06		-0.04
9	33	F	L	0.12			
10	33	M	R	0.3	0.02		
11	32	F	L	-0.06	-0.06	-0.04	-0.08
12	44	F	L	0	-0.08	-0.06	0.02
13	30	F	L	1.46	0.04	-0.04	0.02
14	43	F	R	1.62			
15	38	M	R	0.02	-0.14	-0.06	0.04
16	31	F	L	1	0.02	0	0
17[b]	33	M	L	1.7	1.26	0.34	0.28
18	41	F	R	1.7	0.04	-0.1	-0.1
19	42	F	R	0.22	0	0.02	-0.08
20	30	F	R	-0.06	-0.18	-0.06	-0.12

21	34	F	R	1.6	0.18	0.22	0.22
22	26	F	L	1.44	1	1.06	0.92
23	34	F	L	0.42	0.1	0.08	0.02
24	24	F	R	0.32	0	0.02	0.02
25	23	F	R	0.66		0.28	0.22
26	30	F	R	1.7	0.06	0	-0.06
27	35	F	R	1.08	0.22	-0.04	0.02
28	25	M	L	1.7	0.54	0.32	0.26
Patients	Mean 32	5M 23F	14R 14L	0.72 (SD 0.69)	0.16 (0.35)	0.11 (0.25)	0.09 (0.22)
Controls	Mean 30	2M 8F					

[a]This patient had a recurrence of mild ON in the fellow eye at three months (worst logMAR 0.3), from which she recovered well (logMAR -0.08 by the six month time-point), and was included in the analysis. [b]This patient had coexistent bilateral keratoconus with best corrected acuity of 0.18, and was included in analyses which included fellow eye acuity as a covariate, but excluded when looking at predictors in which recovery was classified purely on the basis of affected eye logMAR, without entering the fellow eye as a covariate.

SD=standard deviation

Table 2. Longitudinal changes in structural and electrophysiological measures in patients and controls

PATIENTS		Baseline mean (95%CI)	3 months mean (95%CI)	6 months mean (95%CI)	12months mean (95%CI)	Change from baseline to 12 months P value
OPTIC NERVE	**FSE lesion length (mm)[a]**	**22.07 (18.35-25.79)**	**24.82 (20.98-28.66)**	**29.82 (25.92-33.72)**	**31.26 (27.28-35.23)**	**<0.001**
	Gad lesion length (mm)	23.54				-
	Area ratio (Affected: Fellow)	**1.19 (1.13-1.24)**	**1.01 (0.94-1.07)**	**1.00 (0.93-1.06)**	**0.89 (0.82-0.95)**	**<0.001**
OPTIC RADIATIONS	**Lesion load (mm^2)**	63 (3-123)	85 (25-146)	**102 (41-162)**	**118 (57-179)**	**<0.001**
	FA[b]	0.36 (0.34-0.37)	0.36 (0.34-0.37)	0.35 (0.34-0.37)	0.36 (0.34-0.38)	0.693
OCCIPITAL CORTEX	Pericalcarine surface area (mm^2)	1212 (1123-1301)	1215 (1124-1307)	1196 (1103-1289)	1218 (1124-1312)	0.836
	Pericalcarine volume (mm^3)	1808 (1666-1950)	1824 (1679-1969)	1764 (1616-1911)	1798 (1650-1946)	0.830
	Pericalcarine cortical thickness(mm)	1.61 (1.57-1.66)	1.61 (1.56-1.66)	1.60 (1.55-1.65)	1.60 (1.55-1.65)	0.441

VISUAL EVOKED POTENTIALS	**Whole field amplitude (μV)**	5.30 (3.97-6.64)	6.57 (5.17-7.98)	**6.67 (5.24-8.09)**	**7.14 (5.68-8.61)**	**0.008**
	Central latency (ms)[c]	123 (115-131)	123 (115-131)	119 (111-127)	**114 (106-122)**	**0.020**
CONTROLS						
OPTIC NERVE	Area ratio	1.03 (0.98-1.07)	1.00 (0.95-1.05)	1.01 (0.96-1.06)	0.97 (0.92-1.03)	0.091
OPTIC RADIATION	FA	0.36 (0.34-0.38)	0.37 (0.35-0.39)	0.37 (0.35-0.40)	0.38 (0.36-0.41)	0.072
OCCIPITAL CORTEX	Pericalcarine surface area (mm^2)	1390 (1241-1538)	1342 (1185-1500)	1376 (1218-1533)	1391 (1233-1548)	0.989
	Pericalcarine volume (mm^3)	2116 (1827-2405)	2066 (1771-2362)	2148 (1853-2444)	2062 (1767-2358)	0.447
	Pericalcarine cortical thickness(mm)	1.63 (1.56-1.70)	1.64 (1.56-1.72)	1.69 (1.61-1.77)	1.60 (1.52-1.68)	0.523

[a]One patient had a subclinical FSE lesion in the fellow nerve

[b]At 3/123 time-points for which data were available, the connectivity of one of the reconstructed optic radiations was too low to survive thresholding, and only the contralateral successfully reconstructed tract was used to estimate the FA.

[c]There were no significant changes over time in whole field VEP latency. Central VEP amplitude increased from baseline to 3 months only (P=0.019).

Significant changes are highlighted in bold font (P<0.05). CI=confidence interval, FA=fractional anisotropy, FSE=fast spin-echo, Gad=gadolinium enhanced MRI, LGN=lateral geniculate nuclei, LOC=lateral occipital complex, V1=primary visual cortex

Table 3. Residual damage at 12 months

	Patients: affected eye	Patients: fellow eye	Controls	Patients vs controls t-tests P values	
				Affected eye	Fellow eye
RNFL (µm)	**79**	100	**106**	**<0.001**	0.167
Macular volume (mm^3)	**6.01**	6.62	**6.82**	**0.001**	0.085
VEP amplitude (µV)	7.2	9.4	9.5	0.054	0.930
VEP latency (ms)	**112**	96	97	**0.020**	0.826

Results of optical coherence tomography and VEP at 12 months are reported for patients' affected and fellow eyes, and controls. Significant changes are in bold (P<0.05). The P values are derived from two-sample unpaired t-tests. RNFL=retinal nerve fiber layer

Table 4. Associations between structural, electrophysiological, functional and demographic variables, and visual outcome (logMAR acuity at 12 months)

	Patient variable	Baseline association with visual outcome P value	12month association with visual outcome P value
RETINA	**Macular volume**	-	**0.045 (r=-0.52)**
	RNFL	-	0.734
OPTIC NERVE	FSE lesion length	0.910	0.505
	Gad lesion length	0.229	-
	Optic nerve area	0.740	0.898
OPTIC RADIATIONS	Lesion load	0.696	0.853
	FA	0.789	0.915
OCCIPITAL CORTEX	Pericalcarine surface area	0.479	0.703
	Pericalcarine volume	0.834	0.627
	Pericalcarine cortical thickness	*0.074*	0.941
VEP	Amplitude	*0.056*	0.575
	Latency	0.267	0.592
fMRI	Affected V1	*0.067*	0.714
	Affected LGN	0.298	0.826
	Affected LOC	**0.007 (r=-0.57)**	0.943

	Affected cuneus	0.240	0.336
	Fellow V1	0.615	0.415
	Fellow LGN	0.725	0.818
	Fellow LOC	**0.020 (r=-0.51)**	0.646
	Fellow cuneus	0.756	0.357
SEVERITY OF BASELINE VISUAL LOSS	**Baseline visual acuity**	**0.014 (r=0.52)**	-
DEMOGRAPHIC	**Age**	**0.040 (r=-0.43)**	-
	Gender	0.653	-
	Side of ON	0.163	-

Significant associations are highlighted in bold. The associated partial correlation coefficient (r) is reported for significant associations in parentheses. FA=fractional anisotropy, FSE= fast spin-echo, Gad=gadolinium enhanced MRI scan, LGN=lateral geniculate nuclei, LOC=lateral occipital complexes, RNFL=retinal nerve fiber layer, V1=primary visual cortex

Table 5. Structure-function interactions during the acute episode: results of multivariable regression modeling

		VARIABLE OF INTEREST			
		fMRI affected LOC BL P value	fMRI fellow LOC BL P value	BL acuity P value	Age P value
BL	**OPTIC NERVE** FSE lesion length	**0.008** *(0.088)*	**0.022** (0.198)	**0.005** **(0.010)**	**0.046** (0.644)
	Gad lesion length	**0.037** (0.148)	**0.042** (0.252)	*0.056* (0.280)	**0.032** (0.544)
	Cross-sectional area	**0.006** *(0.075)*	**0.020** (0.220)	**0.005** **(0.010)**	*0.081* (0.162)
	OPTIC RADIATIONS Lesion load	**0.009** *(0.086)*	**0.017** (0.204)	**0.015** (0.233)	**0.046** (0.644)
	Mean FA	**0.026** (0.156)	**0.039** (0.273)	**0.027** (0.311)	*0.071* (0.213)
	OCCIPITAL CORTEX PC surf. area	**0.010** *(0.080)*	**0.021** (0.210)	**0.042** (0.315)	**0.019** (0.380)
	PC volume	**0.006** *(0.075)*	**0.013** (0.169)	**0.042** (0.315)	**0.016** (0.336)
	PC thickness	**0.002** **(0.028)**	**0.043** (0.215)	**0.036** (0.324)	*0.059* (0.472)
	VEP Amplitude	**0.046** *(0.092)*	0.184 (0.184)	0.140 (0.140)	**0.027** (0.704)
	Latency	**0.043** (0.129)	*0.061* (0.183)	*0.050* (0.300)	**0.044** (0.704)
	FMRI Affected V1	-	-	*0.098* (0.294)	**0.026** (0.494)
	Affected LGN	-	-	**0.027** (0.311)	*0.056* (0.504)
	Affected LOC	-	-	0.131 (0.262)	0.209 (0.209)
	Affected cuneus	-	-	**0.031** (0.310)	*0.062* (0.372)
	Fellow V1	-	-	**0.006** (0.108)	*0.064* (0.320)
	Fellow LGN	-	-	**0.015** (0.233)	**0.046** (0.644)
	Fellow LOC	-	-	*0.097* (0.388)	*0.050* (0.525)
	Fellow cuneus	-	-	**0.004** *(0.084)*	*0.050* (0.525)
	BASELINE ACUITY	*0.079* *(0.079)*	0.181 (0.362)	-	*0.060* (0.420)
	DEMOGRAPHIC Age	**0.036** (0.180)	*0.052* (0.208)	**0.019** (0.247)	-
	Gender	**0.009** *(0.086)*	**0.008** (0.112)	**0.018** (0.252)	**0.049** (0.588)
	Side of ON	**0.021** (0.147)	**0.038** (0.304)	**0.013** (0.221)	*0.068* (0.272)

The variables of interest associated with visual outcome at 12 months are listed in the columns. All baseline variables are listed in the rows. The P values represent the significance of the association between the variable of interest with visual outcome at 12 months, *after adjusting for the interaction variable in that row.* Significant results

are highlighted in bold and weak significance in italics. P<0.05 is considered significant. Holm-corrected P values are reported in parentheses. BL=baseline, FA=fractional anisotropy, gadolinium-enhanced MRI, LGN=lateral geniculate nuclei, LOC=lateral occipital complexes, PC=pericalcarine, V1=primary visual cortex

Table 6. Structure-function interactions with residual damage at 12 months: results of multivariable regression modeling

12M INTERACTION IN	VARIABLE OF INTEREST					
		fMRI affected LOC BL P value	fMRI fellow LOC BL P value	BL acuity P value	Age P value	Macular volume 12M P value
	RETINA Macular volume	**0.039** *(0.098)*	**0.028** (0.182)	0.222 (0.396)	0.342 (0.342)	-
	RNFL thickness	**0.016** (0.144)	*0.090* *(0.090)*	*0.068* (1)	0.234 (0.468)	**0.028** (0.574)
	OPTIC NERVE FSE lesion length	**0.030** (0.150)	**0.007** *(0.077)*	**0.047** (0.799)	*0.089* (0.801)	**0.001** **(0.022)**
	Cross-sectional area	**0.046** **(0.046)**	**0.026** (0.208)	*0.087* (1)	0.119 (0.595)	**0.029** (0.551)
	OPTIC RADIATIONS Lesion load	**0.039** *(0.098)*	**0.021** (0.210)	0.105 (0.840)	*0.079* (0.830)	*0.074* (0.814)
	Mean FA	**0.032** (0.128)	**0.030** (0.150)	0.174 (0.696)	0.114 (0.684)	*0.086* (0.344)
	OCCIPITAL CORTEX PC surf. area	**0.025** (0.175)	**0.031** (0.124)	*0.088* (0.968)	*0.062* (0.992)	**0.045** (0.675)
	PC volume	**0.020** (0.160)	**0.028** (0.182)	*0.086* (1)	**0.049** (0.882)	**0.034** (0.578)
	PC thickness	**0.028** (0.168)	**0.022** (0.198)	0.102 (0.918)	*0.077* (0.924)	*0.083* (0.457)
	VEP Amplitude	**0.007** *(0.070)*	**0.049** *(0.098)*	*0.022* (0.396)	**0.011** (0.209)	**0.041** (0.656)
	Latency	**0.003** **(0.033)**	**0.040** (0.120)	**0.007** (0.133)	*0.071* (0.994)	**0.031** (0.558)
	FMRI Affected V1	-	-	0.144 (0.936)	*0.063* (0.945)	*0.090* (0.270)
	Affected LGN	-	-	0.186 (0.558)	*0.097* (0.776)	*0.076* (0.646)
	Affected LOC	-	-	0.144 (0.936)	0.143 (0.572)	*0.076* (0.646)
	Affected cuneus	-	-	*0.080* (1)	0.111 (0.777)	*0.083* (0.457)
	Fellow V1	-	-	0.295 (0.295)	*0.079* (0.830)	**0.046** (0.644)
	Fellow LGN	-	-	*0.098* (0.980)	*0.076* (0.988)	*0.075* (0.750)
	Fellow LOC	-	-	0.164 (0.820)	0.159 (0.477)	*0.082* (0.574)
	Fellow cuneus	-	-	*0.070* (1)	*0.059* (1)	*0.065* (0.780)
	BASELINE	-	-	-	-	0.152 (0.152)
	DEMOGRAPHIC Age	-	-	-	-	0.109 (0.218)

	Gender	-	-	-	-	*0.055* (0.715)
	Side of ON	-	-	-	-	**0.028** (0.574)

The variables of interest associated with visual outcome at 12 months are listed in the columns. All 12 month variables are listed in the rows. The P values represent the significance of the association between the variable of interest with visual outcome at 12 months, *after adjusting for the interaction variable in that row*. Significant results are highlighted in bold and weak significance in italics. Holm-corrected p values are reported in parentheses. BL=baseline, FA=fractional anisotropy, gadolinium-enhanced MRI, LGN=lateral geniculate nuclei, LOC=lateral occipital complexes, PC=pericalcarine, RNFL=retinal nerve fiber layer, V1=primary visual cortex, 12M=12 months

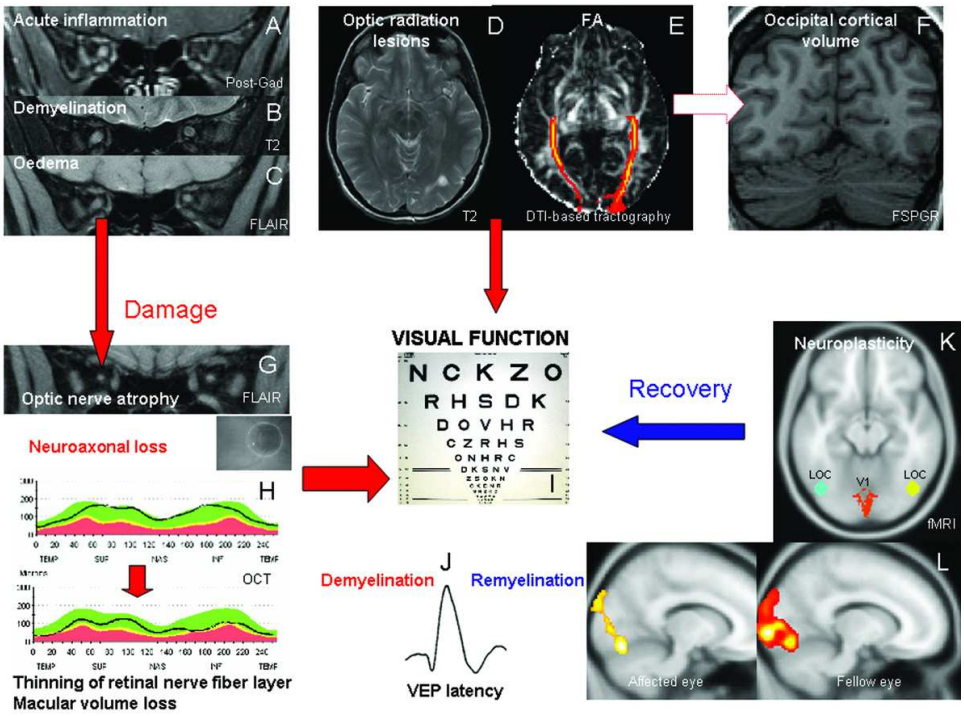

Fig 1. Techniques used to assess mechanisms of damage and recovery in optic neuritis in this study. DTI = diffusion tensor imaging, FA = fractional anisotropy, FLAIR = fluid attenuated inversion recovery, FSE = fast spin-echo, FSPGR = fast spoiled gradient echo, Gad = post gadolinium enhanced MRI, LOC = lateral occipital complex, OCT = optical coherence tomography, V1 = primary visual cortex
52x39mm (600 x 600 DPI)

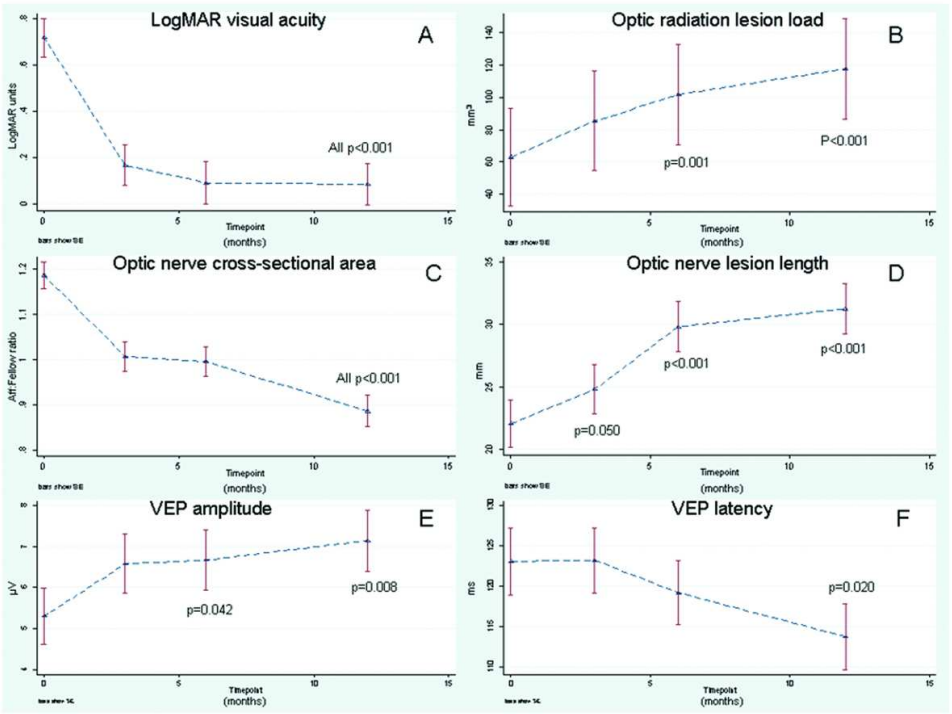

Fig 2. Graphs showing longitudinal changes in (A) visual acuity, (B) optic radiation lesion load, (C) optic nerve cross-sectional area, (D) optic nerve lesion length, (E) VEP amplitude and (F) VEP latency. Significant changes from baseline are indicated by the associated P value. The bars show standard errors. Higher logMAR scores indicate worse acuity.
52x39mm (600 x 600 DPI)

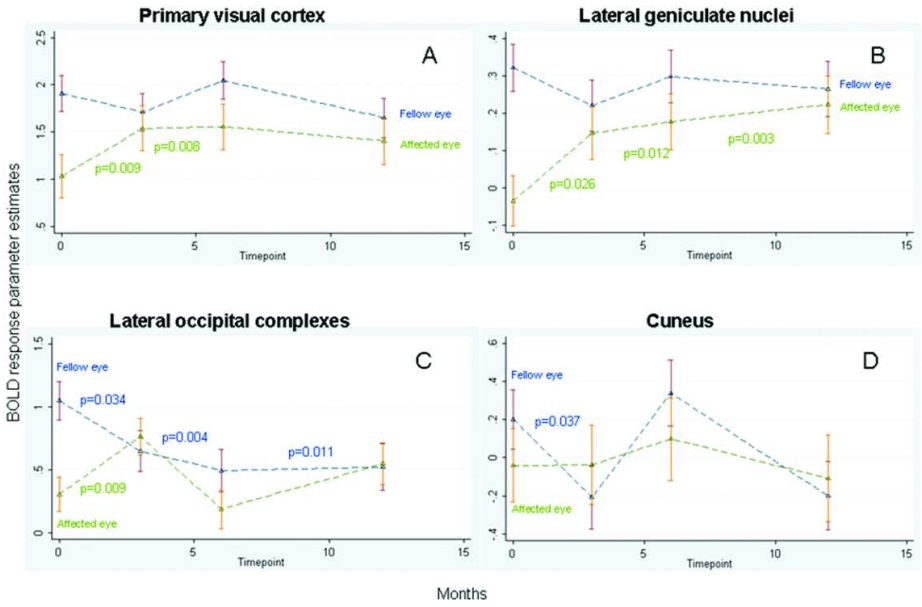

Fig 3. Graphs showing longitudinal changes in fMRI activity, on stimulation of the affected and fellow eyes, in the four regions of interest implicated in neuroplastic responses by previous studies, (A) primary visual cortex, (B) lateral geniculate nuclei, (C) lateral occipital complexes and (D) cuneus. Affected eye responses are plotted in green and fellow eye responses in blue. Significant changes from baseline are indicated by the associated P value. The bars show standard errors. BOLD = blood oxygenation level dependent
52x39mm (600 x 600 DPI)

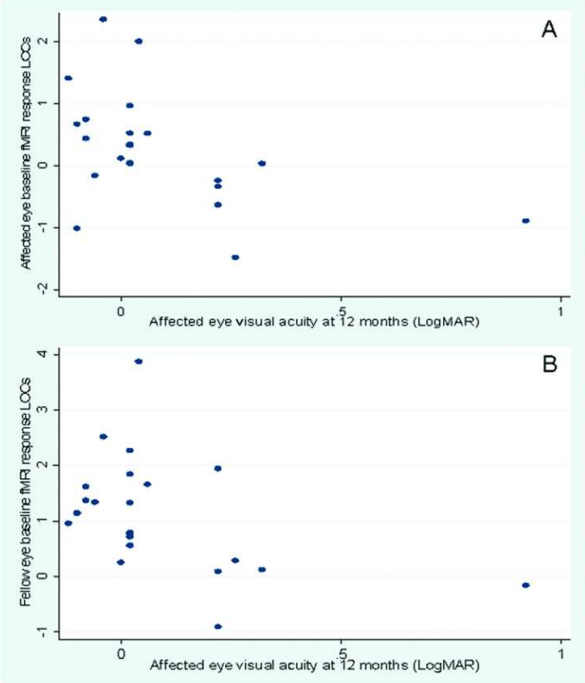

Fig 4. Scatter-plots of affected eye acuity at 12 months against baseline LOC fMRI response on (A) affected and (B) fellow eye stimulation. Higher logMAR scores indicate worse acuity. BOLD = blood oxygenation level dependent, LOC = lateral occipital complexes
52x39mm (600 x 600 DPI)

Supplementary Material

(1) Tractography

A diffusion-based probabilistic tractography algorithm was used to reconstruct the optic radiations (http://www.fmrib.ox.ac.uk/fsl/fdt/fdt_probtrackx.html[26,27]). To define the seed-points in Meyer's loop we used a methodology which is based on the functional data. This approach has been applied before to reconstruct the human motor tracts,[42] and we modified it for application to the visual system. It consisted of the following steps. The locations of the LGNs were first identified functionally, by combining first level fMRI contrast images from all of the subjects for all conditions i.e. right and left eyes, colored and black and white checkerboards, at each time-point. Two spherical regions of interest were created, centered on the global maximal coordinates of each LGN (MNI coordinates 22 -24 -4 for the right LGN, -22 -26 -4 for the left), each of 3.5mm radius, resulting in volumes of 180mm^3. These dimensions were chosen to approximate the published volumes of the LGN, which are of spatulate shape and 5x6x9mm.[43] These were then reverse normalized into each subject's native space, coregistered to each individual's partial brain diffusion data in a two stage procedure, using the whole brain DTI acquisition as an intermediate step, and binarized. Each of these LGN-derived seed masks was then moved 8-10 voxels laterally in each subject's native diffusion space, so that it was located within the apex of Meyer's loops. The maximum number of voxels was always used for this shift, in order to achieve appropriate placement, which was confirmed visually in all cases. The intra-observer coefficient of variation was 0%. This method was used to overcome difficulties tracking round the sharp angle of the loop, and

to track from voxels located in white matter. These regions were used as the seed points for probabilistic tractography.

The target region for the tractography was the primary visual cortex which was outlined in each subject using a previously described methodology.[44] It consisted of manually drawing the visual cortex on the standardized T1 image, that is the individual T1-weighted image coregistered into a standardized space defined by Montreal Neurological Institute (MNI152), using affine transformation, as employed by FMRIb Software Library (FSL).[45] This was done by using, as a guide, a region of interest derived from area 17 in the Brodmann atlas. The visual cortical areas were then transferred back to the individual T1 images, and their correct location was confirmed by visual inspection in all cases. Probabilistic tissue-type segmentation and partial volume estimation were then performed on the individual T1-weighted images.[46] The output images were thresholded, to include only voxels estimated at >30% grey matter, and the results were used to mask the visual cortical areas to obtain the final target masks.

Exclusion masks were placed at the anterior limit of Meyer's loop, and in the sagittal midline, in each subject to constrain the tractography algorithm, which was run using 5000 samples and a curvature threshold of 11.5 degrees. The resulting connectivity maps were thresholded for noise correction, in line with previous brain tractography studies.[42,44,47,48] The thresholded connectivity map was then transformed into a binary image, which was used to mask the anisotropy map to delineate the optic radiation. The mean voxel values of fractional anisotropy (FA) within this tract were obtained for each subject.

(2) FMRI experimental design

The visual stimulation paradigm comprised 16 second epochs of flickering checkerboard stimulation, alternated with 16 second epochs of grey background, presented on a projection screen. Subjects were instructed to fixate a central fixation cross, present during both conditions, which changed intermittently to a # symbol. They wore transparent plano chromatic filter goggles, with one green and one red filter (Haag-Streit, UK). The checkerboards were also green and red, so that the green checkerboard was invisible through the red filter, and likewise for the red checkerboard through the green filter. This was to allow monocular stimulation whilst testing both eyes within the same run, and to enable the subjects to fixate the cross with at least one eye, even in cases of severe monocular visual loss. Confirmation of attention and fixation was facilitated in this manner.[32]

Each session consisted of eight epochs of checkerboard stimulation (four right eye and four left eye presented in a pseudo-randomized order), alternated with eight epochs of background. Each experiment consisted of two sessions, and the orientation of the goggles was reversed in between, in order to swap the red and green filters.

After this, the subjects had two sessions of stimulation using black and white checkerboards, one for each eye, with the fellow eye patched. Each of these sessions consisted of four epochs of stimulation alternated with four of rest, each epoch again of 16 seconds duration. These data were only used to help functionally define the LGN as a region-of-interest, and seed-mask for tractography.

The rectangular projection screen covered 30 degrees of visual angle horizontally and 28 degrees vertically, at a viewing distance of 57cm. The borders of the checkerboard squares were radii 10 degrees apart. The size of the squares increased with distance from

the centre in a linear manner, consistent with the cortical magnification factor.[49] The luminances of the checkerboards were approximately equal: 1.32 cd/m^2 for the green checkerboard, and 1.23 cd/m^2 for the red. The chromaticities of the checkerboard stimuli were as follows: 0.31 red and 0.46 green comprising the green checkerboard, and 0.44 red and 0.34 green comprising the red checkerboard. These values were decided by several observers to be the optimally filtered wavelengths when viewed through the opposite color goggle. Checkerboard reversal frequency was 8 Hz.

(3) Specification of regions-of-interest for fMRI data extraction

For primary visual cortex, the region was specified utilizing a Brodmann area 17 normalized target mask, which was also used as the target mask for tractography of the optic radiations.

LGN data were extracted using seed masks derived from the group fMRI data, combining checkerboard stimulation through the goggles (and also the two sessions of black and white checkerboard stimulation), for both affected and fellow eyes, from all patients and controls. As the LGN receive afferent input from both eyes, data was averaged for the left and right sides.

Our study did not include a localizer task to identify the LOCs, so instead we constructed 1cm^3 spherical regions of interest centered on their average reported coordinates from previous studies (+/-43, -70, -13),[10,12] a methodology used by previous investigators.[12] Data was again averaged for the two LOCs, as they receive bilateral neural input.

The cuneus was selected as a fourth region of interest because it had been identified as a potential site for plasticity in a previous baseline cross-sectional fMRI analysis, derived

from this patient cohort.[50] A significant cluster of 580 voxels with global maximum at -10 -84 32 ($p<0.05$ corrected) was identified, which correlated with better visual acuity in the acute phase, after correcting for significant structural predictors and demographics. This suggested that it might be a site for plastic responses, and we were therefore interested investigating longitudinal changes in this region, which represents the dorsal stream. Data was extracted using a mask derived from this cluster.

(4) Patient adherence

[a]The reasons for the missing visits were as follows: three patients and two controls decided they did not want to continue in the study after the first visit, and a further one patient after the second visit. Five patients became pregnant during the study, three missing MRI at 12 months, one MRI at six and 12 months, and one MRI at six months. One patient missed the three month visit due claustrophobia in the scanner, but decided subsequently to return. Four of the five pregnant patients attended for clinical assessment, VEPs and OCT.

For the analysis in which the clinical utility of fMRI as a baseline predictor was evaluated, data was available for 23/28 patients. This included one patient who had recovered well at three months and was then lost to follow-up. Visual outcome data was not available for three patients who were lost to follow-up. FMRI data was not available at baseline for another (see footnote f in this section), and the patient with coexistent keratoconus was excluded from this analysis (see Table 1, footnote b).

[b]None of the controls had Gad-enhanced MRI, and two patients declined intravenous injections.

[c]Sequence unavailable, due to time-constraints, or technical failure.

[d]OCT became available on-site during the course of the study. Therefore, six patients who had already passed the 12 month time-point, and one control, did not have an OCT examination. In total, 9/10 controls had OCT and 18/24 patients with longitudinal follow-up had OCT, at the 12M time-point only.

[e]Controls were only assessed with VEP and OCT on one occasion.

[f]In one patient at baseline, and two patients at 12 months, a parameter estimate for LOC extraction was unobtainable, due to temporal signal dropout.

[g]Patients had all their tests on the same day in 81% of time-points, and within two days in 88% of cases. In the remainder, the median delay was 10.5 days. At baseline, there were three delays of 5, 5 and 21 days, with the delayed tests structural MRI, structural MRI and VEP, and fMRI respectively. All analysis was repeated excluding the patient with a 21 day delay, and the results were materially unaffected.

Table S1. Longitudinal dataset

	Baseline	**3 months**	**6 months**	**12 months**
No. patients attending	28	24[a]	23	24
No. controls attending	10	8[a,e]	8	8
No. of optic nerve FSE acquired	38	32	30	28[a]
No. of optic nerve Gad acquired	26[b]			
No. of optic nerve FLAIR acquired	38	32	30	28
No. of brain FSPGR acquired	38	32	29[c]	28
No. of brain FSE acquired	38	32	30	28
No. of DTI OR acquired	37[c]	32	29[c]	25[c]

No. of OCT acquired				27[d]
No. of VEP acquired	38	24[e]	23	21
No. of fMRI acquired	38	32	30	28[f]
No. of patients with a delay between tests of >2 days[g]	3	2	3	4

The number of participants who had each test, at each time-point, is reported. For explanations to the superscripts, see Supplementary Material (4): Patient adherence. DTI=diffusion tensor imaging, FLAIR=fluid attenuated inversion recovery, FSE=fast spin-echo, FSPGR=fast spoiled gradient echo, Gad=gadolinium-enhanced MRI scan, OCT=optical coherence tomography, OR=optic radiations